We are IntechOpen, the world's leading publisher of Open Access books
Built by scientists, for scientists

6,900
Open access books available

185,000
International authors and editors

200M
Downloads

154
Countries delivered to

Our authors are among the

TOP 1%
most cited scientists

12.2%
Contributors from top 500 universities

CLARIVATE ANALYTICS
BOOK CITATION INDEX
INDEXED

WEB OF SCIENCE™

Selection of our books indexed in the Book Citation Index
in Web of Science™ Core Collection (BKCI)

Interested in publishing with us?
Contact book.department@intechopen.com

Numbers displayed above are based on latest data collected.
For more information visit www.intechopen.com

Thermoelectric Effect and Application of Organic Semiconductors

Nianduan Lu, Ling Li and Ming Liu

Additional information is available at the end of the chapter

Abstract

Human development and society progress require solving many pressing issues, including sustainable energy production and environmental conservation. Thermoelectric power generation looks like promising opportunity converting huge heat from the sun and waste heat from industrial sector, housing appliances and infrastructure and automobile and other fuel combustion exhaust directly to electrical energy. Thermoelectric power generation will be of high demand, when technology will be affordable, providing low price, high conversion efficiency, reliability, easy applicability and advanced ecological properties of end products. In this context, organic thermoelectric materials attract great interest caused by non-scarcity of raw materials, non-toxicity, potentially low costs in high-scale production, low thermal conductivity and wide capabilities to control thermoelectric properties. In this chapter, we focus mainly on thermoelectric effect in several organic semiconductors, both crystalline and disordered. We present theory of some transport phenomena determining thermoelectric properties of organic semiconductors, including general expression of thermoelectric effect, percolation theory of Seebeck coefficient, hybrid model of Seebeck coefficient, Monte Carlo simulation and first-principle theory. Finally, a future outlook of this field is briefly discussed.

Keywords: organic semiconductor, thermoelectric effect, theoretical model

1. Introduction

1.1. Organic semiconductors

1.1.1. History

Organic semiconductors have revealed promising performance and received considerable attentions due to large area, low-end, lightweight and flexible electronics applications [1]. Currently, organic semiconductors have appealed for a broad range of devices including sensors, solar cells, light-emitting devices and thermoelectric application [2, 3]. Historically, organic materials were

viewed as insulators with applications commonly seen in inactive packaging, coating, containers, moldings and so on. The earliest research on electrical behavior of organic materials dates back to the 1960s [4]. In the 1970s, photoconductive organic materials were recognized and were used in solar cells and xerographic sensors, etc. [5]. In about the same age, organic thermoelectric materials, such as conducting polymers, had been investigated [6], although First European Conference on Thermoelectric in 1988 had no mention of organic materials in their proceeding. Since proof of concept for organic semiconductors occurred in the 1980s, remarkable development of organic semiconductors has promoted improvement of performance that maybe competitive with amorphous silicon (a-Si), increasing their suitability for commercial applications [7]. Appearance of conductive polymers in the late 1970s, and of conjugated semiconductors and photoemission polymers in the 1980s, greatly accelerated development in the field of organic electronics [8]. Polyacetylene was one of the earliest polymer materials known to be potential as conducting electricity [9], and one could find that oxidative dopant with iodine could greatly increase conductivity by 12 orders of magnitude [10]. This discovery and development of highly conductive organic materials were attributed to three scientists: Alan J. Heeger, Alan G. MacDiarmid and Hideki Shirakawa, who were jointly awarded the Nobel Prize in Chemistry in 2000 for their discovery in 1977 and development of oxidized, iodine-doped polyacetylene. After that, plenty of organic semiconductor materials were synthesized, and research field of organic electronics matured over the years from proof-of-principle phase into major interdisciplinary research area, involving physics, chemistry and other disciplines. As important branch of organic semiconductors, in the past decade, organic thermoelectric effect has received much attention. **Figure 1** shows Thomson Reuters Web of Science publication report for the topic "organic thermoelectric Seebeck effect" for the last 16 years [3]. Research interest in organic thermoeletrics Seebeck effect has been growing remarkably over the last 5 years.
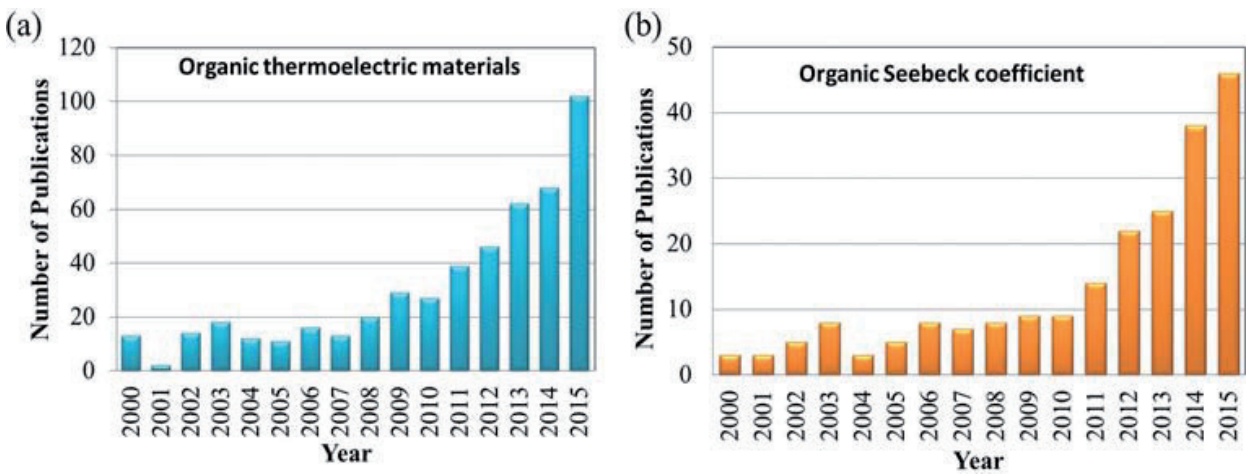

Figure 1. Thomson Reuters web of science publication report for the topic "organic thermoelectric Seebeck effect" from 2000 to 2015.

1.1.2. Structure

Organic semiconductors can be usually classified as two types: crystalline and amorphous materials, in terms of crystalline fraction (also static disorder) [3, 11].

All organic semiconductor materials are generally characterized by weak van der Waals bonding, which leads to weak intermolecular interactions. This weak coupling of molecules would induce weak interaction energy to give narrow electronic bandwidths. Otherwise, existing narrow electronic bands will be eliminated by statistical variation of width in energy level distribution of molecules, which, hence, creates Anderson charge localization. For crystalline organic semiconductor materials, localization of charge carriers is attributed to intermolecular thermal fluctuations (dynamic disorder), at which size of localized wave function is expected to be on the order of molecular spacing and charge carrier transport in this weakly localized field is treated as "intermediate hopping transport regime" [12]. Because of high density of crystal imperfections in disordered organic semiconductors, such as impurities, grain boundaries, dangling bonds and periodicity loss of crystal, localization of charge carriers is attributed to spatial and energetic disorder due to weak intermolecular interactions [13]. Disorder in organic semiconductors results in basic charge transport mechanism, common for very rich variety of such materials [14], incoherent tunneling (hopping) of charge carriers between localized states [15].

1.2. Charge transport mechanism in organic semiconductors

1.2.1. Dispersive transport

Charge carriers are always slowing down during conduction processes in dispersive transport regime. It happens only when charge carriers' distribution is thermally nonequilibrium. In dispersive transport regime, energy fluctuations allow release (emission) of charge carrier captured by localized state (trap), when state (trap) becomes temporarily shallow during fluctuations [16]. Otherwise, charge carrier release time is strongly dependent on both temperature and energy. Charge carriers localized on shallow states are usually released before the states can change their energies noticeably. In contrast, charge carriers, always being trapped in energetically deeper and deeper states, have to perform longer and longer tunneling transitions to hop to the next destination site. As a result, temperature-dependent distribution of effective activation energies just follows the density of states (DOS) function within domain of shallow states, while these distributions appear to be very different for deep traps.

1.2.2. Nearest-neighbor hopping

Transport in disordered organic semiconductors is generally characterized by charge carrier's localization and hopping transport mechanism [17]. Localized states, randomly distributed in energy and space, form discrete array of sites in hopping space. The most probable hop for charge carrier on site with particular energy is to the closest empty site, that is, to its nearest-neighbor site in hopping space. In conjunction with hopping probability rate, it gives mobility for carriers at this energy. In a word, nearest-neighbor hopping describes hopping regime, in which tunneling part of hopping rates in Eq. (1) referred as hopping rates of Miller-Abrahams is so much slower than energy contribution, that only the nearest neighbors are addressed in hops [18]:

$$\gamma_{ij} = \nu_0 \times \exp\left(-R\right) = \nu_0 \times \begin{cases} \exp\left(-2 \times \alpha \times R_{ij} - \dfrac{E_j - E_i}{k_B T}\right), & E_j - E_i > 0, \\ \exp\left(-2 \times \alpha \times R_{ij}\right), & E_j - E_i < 0 \end{cases} \tag{1}$$

where ν_0 is attempt-to-jump frequency, R is hopping range, α is inverse localized length describing extension of wave function of localized state, R_{ij} is distance between site i and site j, E_i and E_j are energies of sites i and j, respectively. As long as charge carrier can find shallow and empty sites with energies below its current state, it will perform nearest-neighbor hopping to energetically lower sites, since in this case rates are limited by spatial tunneling distances only.

1.2.3. Variable-range hopping

Variable-range hopping (VRH) theory was first proposed by Neville Mott in 1971 [19] and hence was called Mott VRH, which is model describing low temperature conduction in strongly disordered systems with localized states. VRH transport has characteristic temperature dependence of 3D electrical conductance:

$$\sigma = \sigma_0 \times \exp\left[-\left(\frac{T_0}{T}\right)^{1/4}\right], \tag{2}$$

here $k_B T_0 = \frac{\beta}{g(E_f) \times \alpha^3}$, σ_0 is prefactor, α^{-1} is localization length, k_B is Boltzmann constant, $g(E_f)$ is DOS function at Fermi energy E_f, and β is constant coefficient with value in interval 10.0–37.2 according to different theories.

For 3D electrical conductance, and in general for d-dimensions, VRH transport is expressed as:

$$\sigma = \sigma_0 \times \exp\left[-\left(\frac{T_0}{T}\right)^{1/(d+1)}\right], \tag{3}$$

here d is dimensionality.

1.2.4. Multiple trapping and release theory

Multiple trapping and release theory assume that charge carrier transport occurs in extended states, and that most of charge carriers are trapped in localized states. Energy of localized state is separated from mobility edge energy. When localized state energy is slightly lower mobility edge, then localized state acts as shallow trap, from which charge carrier can be released (emitted) by thermal excitations. But, if that energy is far below mobility edge energy, then charge carrier cannot be thermally excited (emitted). In multiple trapping and release theory, total charge carriers' concentration n_{total} is equal to sum of concentrations n_e in extended states and in localized states as in Ref. [20]:

$$n_{total} = n_e + \int_{-\infty}^{0} g(E)f(E)dE, \tag{4}$$

where $f(E)$ is Fermi-Dirac distribution function.

2. Organic thermoelectric materials

2.1. Polymer-based thermoelectric materials

Polymers as thermoelectric materials recently have attracted much attention due to easy fabrication processes and low material cost [21, 22], as well as, low thermal conductivity, which is highly desirable for thermoelectric applications. Different types of polymers have been used in thermoelectric devices [23–25], such as polyaniline (PANI), poly(p-phenylenevinylene) (PPV), poly(3,4-ethylenedioxythiophene) (PEDOT), tosylate(tos), poly(styrenesulfonate) (PSS), and poly(2,5-dimethoxy phenylenevinylene) (PMeOPV), poly[2-methoxy-5-(2-ethylhexyloxy)-1,4-phenylenevinylene] (MEHPPV) and poly(3-hexylthiophene-2,5-diyl) (P3HT). **Figure 2** shows chemical structure of some polymers. These polymers are chosen as thermoelectric materials for their conductive nature. Takao Ishida's group has reported high power factor (PF) values of over 100 $\mu W/(m\ K^2)$ on PEDOT films through chemical reduction with different chemicals in their review [25], as shown in **Table 1**.

Thermoelectric properties of 1,1,2,2-ethenetetrathiolate(ett)–metal coordination polymers poly [Ax(M–ett)] (A = Na, K; M = Ni, Cu) also have been studied, as shown in **Figure 3a** [26]. P-type poly[Cux(Cu–ett)] exhibited best ZT of 0.014 at 380 K with electrical conductivity of ~15 S/cm, Seebeck coefficient of 80 $\mu V/K$ and thermal conductivity of 0.45 W/(m K); n-type poly[Kx(Ni–ett)] showed best ZT of 0.2 at 440 K with electrical conductivity of ~60 S/cm, Seebeck coefficient of 150 $\mu V/K$ and thermal conductivity of 0.25 W/(m K). Otherwise, thermoelectric module based on p-type poly[Cux(Cu–ett)] and n-type poly[Nax(Ni–ett)] (i.e., ZT of 0.1 at 440 K) was built (**Figure 3b** and **c**). More recently, Pipe et al. reported thermoelectric measurements of PEDOT: PSS with 5% of dimethylsulfoxide (DMSO) and ethylene glycol (EG) after submerging films in EG several times (from 0 to 450 min) [27]. Insulating polymer (PSS) is removed, and consequently, electrical conductivity and Seebeck coefficient increase simultaneously. ZT value of 0.42 reported in Pipe et al.'s work is the highest ever obtained for polymer until date.
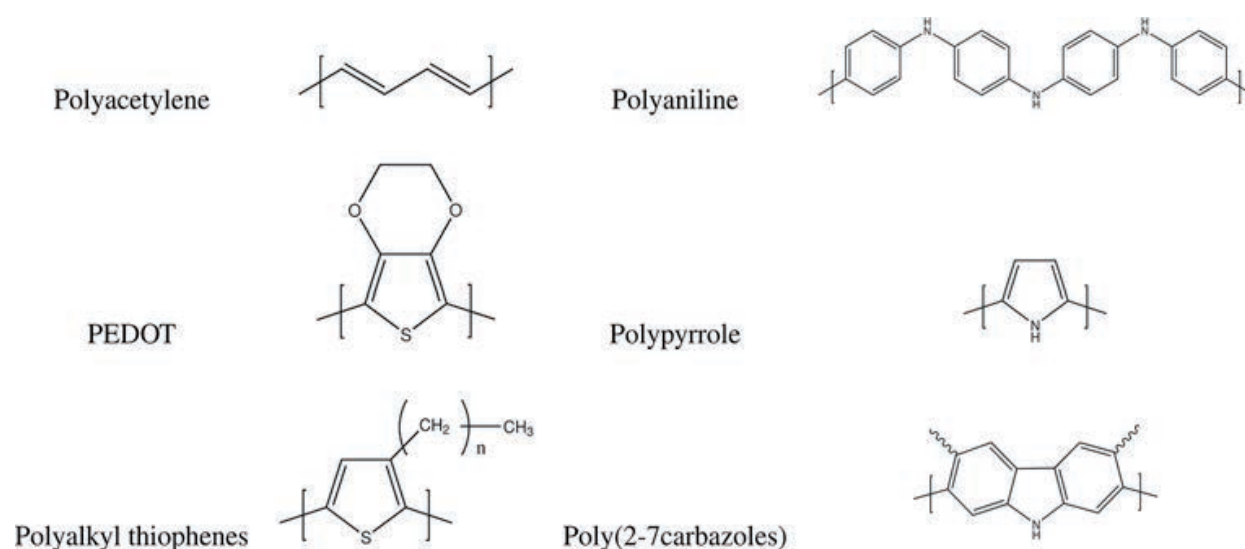

Figure 2. Molecular structures of some typical polymers [23].

Materials	S (μV/K)	PF (μW/m K^2)	ZT
PEDOT:PSS	22	47	0.1
PEDOT:tos (dedoped)	200	324	0.25
PEDOT:PSS	73	469	0.42
PEDOT:tos	~85	12,900	–
PEDOT:tos	55	453	–
PEDOT:BTFMS	~40	147	0.22
PEDOT:PSS (dedoped)	~50	112	0.093
PEDOT:PSS (dedoped)	43	116	0.2
PEDOT:PSS	65	355	~0.3

Table 1. Thermoelectric properties of polymer-based materials (tos: tosylate, and PSS: poly(stryrenesulfonate) [25].
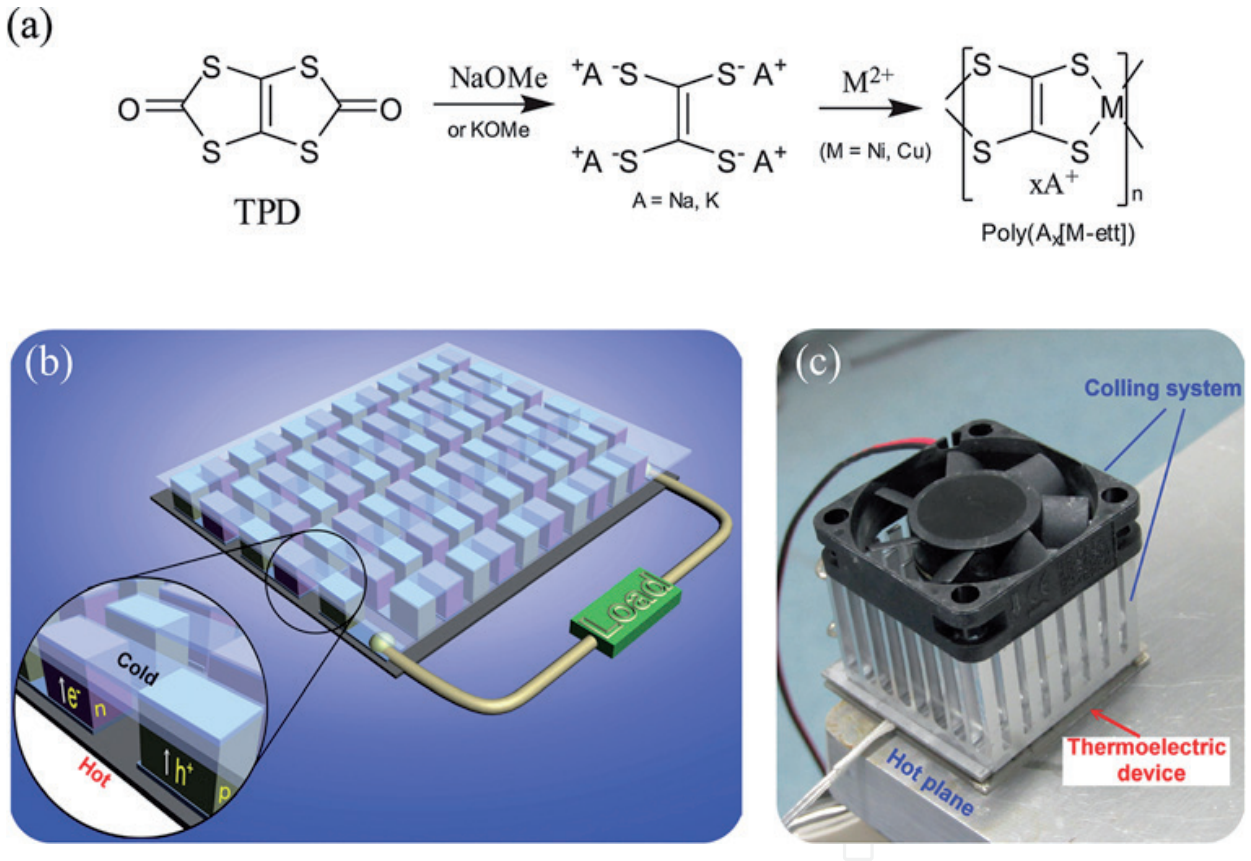

Figure 3. (a) Synthetic route of poly[Ax(M-ett)]s, (b) module structure and (c) photograph of module and measurement system with a hot plane and cooling fan.

Although thermoelectric performance of organic semiconductors has been increased by using different fabricated methods or dopant, as compared with inorganic thermoelectric materials, organic thermoelectric materials still exhibit lower ZT so far. Nevertheless, researchers are making their great efforts in organic semiconductors instead of inorganic materials, due to several more advantages in organic thermoelectric materials, for example, the non-scarcity of raw materials, non-toxicity and large area applications.

2.2. Small molecule-based thermoelectric materials

Currently, investigation of small molecule-based organic thermoelectric materials is lagging behind that of polymers-based organic materials. However, small molecule-based organic thermoelectric materials exhibit plenty of attractions. For example, small molecules are easier to be purified and crystallized and may be more feasible to achieve n-type conduction. **Figure 4** shows chemical structures of some small molecules studied as organic thermoelectric materials [24].

As the benchmark of p-type organic semiconductors, pentacene is the best-known small molecule studied for organic thermoelectric applications. A remarkable attraction for pentacene is attributed to its high mobility up to 3 cm^2/V s in thin film transistors (TFT). Due to low charge carriers' concentration of pentacene in neutral state, appropriate doping treatment is critical to optimization of its thermoelectric properties. So far, F_4TCNQ and iodine are efficient dopant for pentacene [24]. F_4TCNQ is strong electron acceptor that is frequently used as p-type dopant in organic electronics [28]. Harada et al. have achieved maximum electrical conductivity of 4.1 $\times$ 10^{-2} S/cm and maximum PF of 0.16 $\mu W/(m\ K^2)$ by using dopant of 2.0 mol.%, as shown in **Figure 5a**. Furthermore, when thickness of pentacene layer was varied, electrical conductivity could be optimized, while Seebeck coefficient was unaffected (around 200 $\mu V/K$). Finally, maximum PF of 2.0 $\mu W/(m\ K^2)$ was obtained in 6-nm-thick pentacene sample, as shown in **Figure 5b**. For using iodine dopant, Minakata et al. have achieved highest electrical conductivity of 60 S/cm with Seebeck coefficient in the range of 40–60 $\mu V/K$ [29]. As a result, the highest PF is 13 $\mu W/(m\ K^2)$, which is more than six times that of pentacene/F_4TCNQ bilayer sample. In a word, as compared with polymer-based thermoelectric materials, small molecule-based materials are relatively less explored and need to put in more effort in the future.
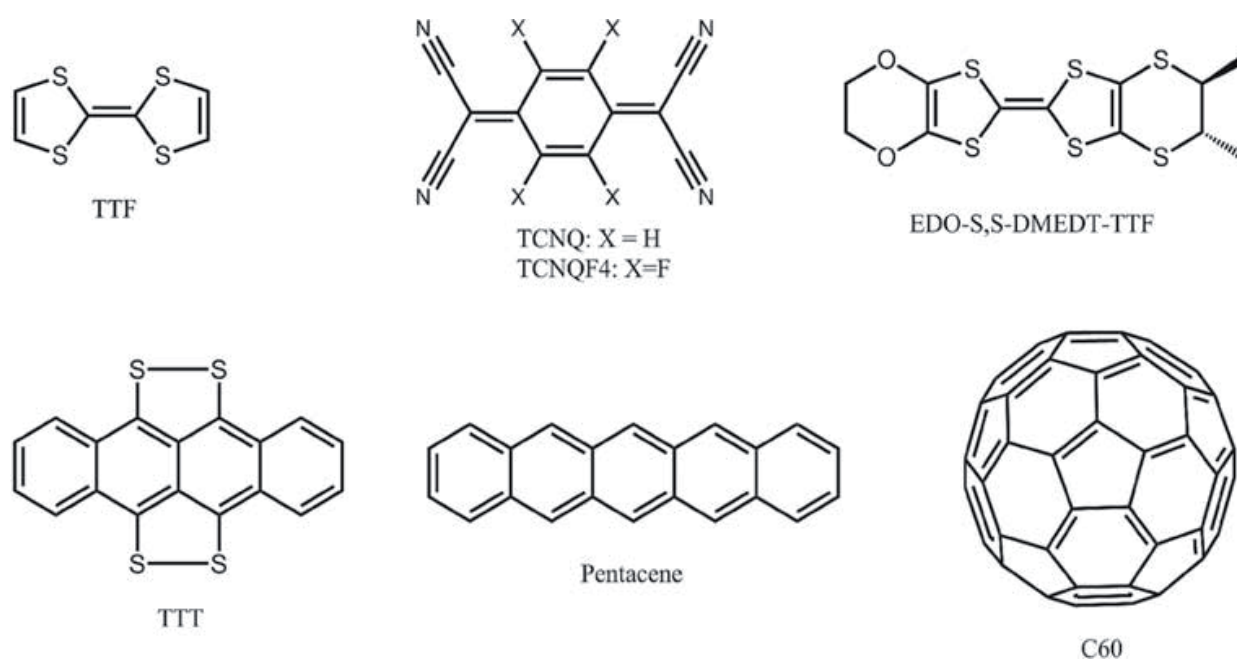

Figure 4. Chemical structures of some small molecules studied as organic thermoelectric materials.
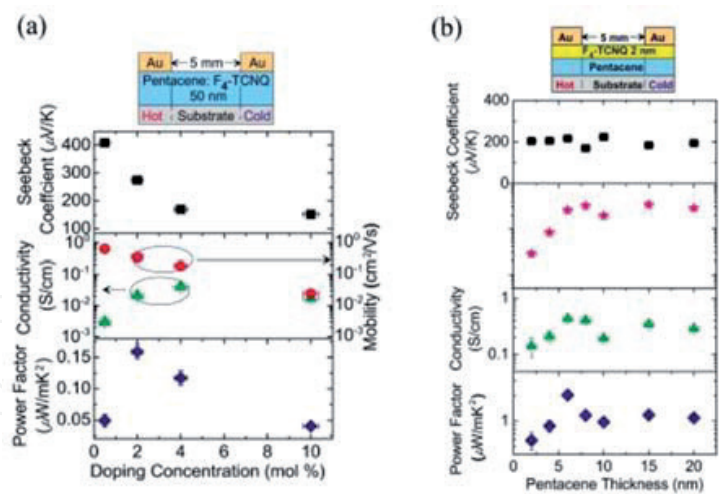
Figure 5. Thermoelectric properties of pentacene samples doped by (a) co-evaporation with F_4TCNQ and (b) forming pentacene/F_4TCNQ bilayer structures.

3. Thermoelectric transport theory of organic semiconductors

3.1. General expression of thermoelectric effect

Since organic semiconductors consist of amorphous and crystal structure, theoretical model of charge carrier thermoelectric transport should be more general. Derivation of present expression of thermoelectric effect was inspired by work of Cutler and Mott [30]. Basic expression was in terms of electrical conductivity σ. Based on definition of Cutler and Mott, for hopping system in disordered lattice at zero and finite temperature, σ was expressed as:

$$\sigma = -\int \left[\sigma_E \frac{\partial f}{\partial E} \right] dE. \tag{5}$$

Otherwise, one can start out by writing electrical conductivity as integral over single states neglecting electron correlation effects [31]:

$$\sigma = e \int g(E)\mu(E)f(E)[1-f(E)]dE. \tag{6}$$

Then, energy dependence of electrical conductivity is written as:

$$\sigma(E) = eg(E)\mu(E)f(E)[1-f(E)], \tag{7}$$

here $g(E)$ is density of states, $\mu(E)$ is mobility, and $f(E)$ is Fermi-Dirac distribution function. Seebeck coefficient S is related to Peltier coefficient Π as follows:

$$S = \frac{\Pi}{T}. \tag{8}$$

Peltier coefficient Π is energy carried by electrons per unit charge. Carried energy is characterized connected with Fermi energy E_f. Contribution to Π of each electron is in proportion to its

correlative contribution to total conduction. Weighting factor for electrons in interval dE at energy E is thus $\frac{\sigma(E)}{\sigma}dE$, with energy dependence of conductivity $\sigma(E)$ as Eq. (7). Therefore, one can obtain general expression of Seebeck coefficient as [32]:

$$S = \frac{-k_B}{e}\int\left(\frac{E-E_f}{k_BT}\right)\frac{\sigma(E)}{\sigma}dE. \qquad (9)$$

To distinguish crystalline solids, general Seebeck coefficient also can be defined as shape of transport energy with mean energy of conducting charge carriers as in Ref. [33]:

$$S = -\frac{1}{eT}\times(E_{trans}-E_f), \qquad (10)$$

where transport energy E_{trans} is defined as averaged energy weighted by electrical conductivity distribution:

$$E_{trans} = \int E\frac{\sigma(E)}{\sigma}dE. \qquad (11)$$

Usual expression of Seebeck coefficient was used early in doped organic materials by Roland Schmechel in 2003 [33]. In Schmechel's article, a detailed method to complex hopping transport in doped system (p-doped zinc-phthalocyanine) was proposed and used to discuss experimental data on effect of doping on conductivity, mobility and Seebeck coefficient.

3.2. Percolation theory of Seebeck coefficient

Percolation theory is considered as the best way known to analytically investigate charge carriers hopping transport characteristics. Percolation problem for charge carriers transport properties in disordered semiconductors has been argued early by Ziman and a number of researchers [34, 35], at which charge transport should be in proportion to percolation probability $P(p)$. A simple definition is that approximates firstly electrical conductivity as [36]:

$$\sigma(E) = \sigma_0 \times P(p(E)), \qquad (12)$$

where $P(p)$ percolation probability is fraction of the volume allowed, but not isolated, and σ_0 denotes a large allowed value of the material. $P(p)$ is known to vanish for p less than critical value B_c, but drops sharply to zero as $p \to B_c$. To make percolation question simple, researchers have put forward two kinds of standpoints for critical B_c, that is, $B_c = 1$, and $B_c = 2.8$ or $B_c = 2.7$. Although researchers have not achieved unified agreement, percolation theory in hopping system was generally established to explain charge carrier transport characteristics.

Generally speaking, charge carrier transport is described by a four-dimensional (4D) hopping space, including three spatial coordinates and one energy coordinate, at which probability of charge carrier hopping between localized sites associated with these four coordinates. Therefore, charge carrier transport would be more complex based on percolation approach addressing, if all of positions, that is, spatial positions of sites and their energies and

occupation of sites, must be included. In Eq. (12), to simulate electrical conductivity $\sigma(E)$, the key is to seek out percolation path in hopping space. Thus, a random resistor network linking all of molecular sites under percolation model is essential. **Figure 6** shows schematic diagram of charge carrier transport in hopping system and corresponding percolation current through polymer matrix for charge carrier to travel through [37].
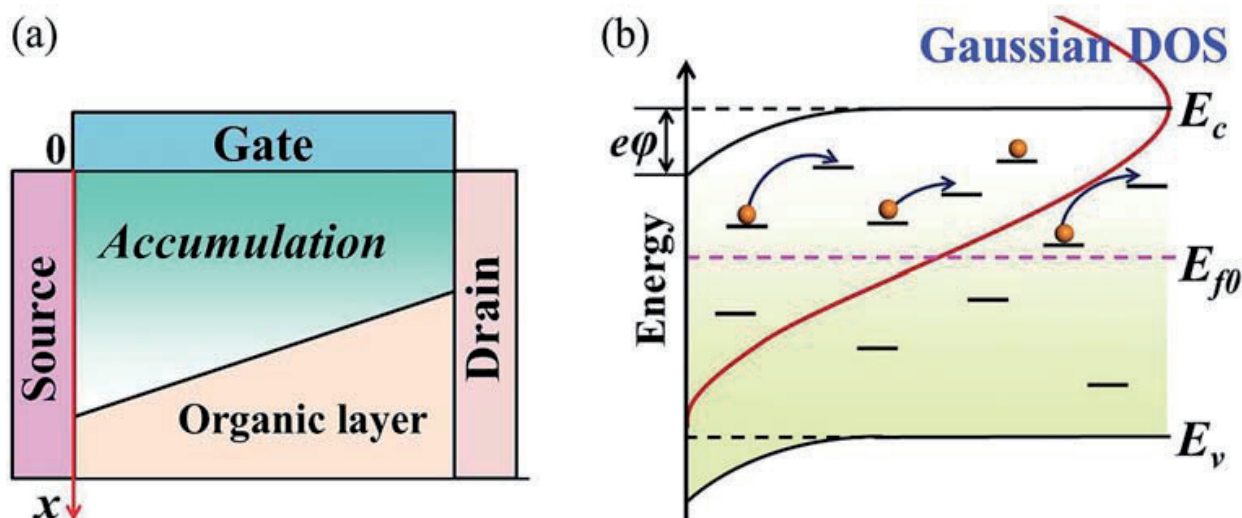

Figure 6. (a) Schematic diagram of charge carrier transport in hopping space with density of states and (b) corresponding percolation current in disordered organic semiconductor.

Based on the following general definition through Kelvin-Onsager relation to Peltier coefficient Π, percolation theory to calculate Seebeck coefficient S in hopping transport is expressed as in Eq. (8), where Π is generally identified with average site energy on percolation cluster and can be written as:

$$\Pi = \int E_i P(E_i) dE_i, \tag{13}$$

where $P(E_i)$ is probability that site of energy E_i is on current-carrying percolation cluster and was further given by:

$$P(E_i) = \frac{g(E_i)P_1(Z_m|E_i)}{\displaystyle\int_{-E_m}^{E_m} g(E_i)P_1(Z_m|E_i)dE}, \tag{14}$$

where $g(E_i)$ is density of states per unit volume, E_m is maximum site energy, and $P_1(Z_m|E_i)$ is probability that second smallest resistance emanating from site with energy E_i is not larger than maximum resistance on percolation cluster Z_m. Expression of probability $P_1(Z_m|E_i)$ is written as:

$$P_1(Z_m|E_i) = 1 - \exp\left[-P(Z_m|E_i)\right] \times \left[1 + P(Z_m|E_i)\right], \tag{15}$$

where $P(Z_m|E_i)$ is bonds' density, which means average number of resistance of Z_m or less connected to site energy E_i. To calculate Peltier coefficient (or Seebeck coefficient), an expression for $P(Z_m|E_i)$ is necessary.

Based on percolation theory, disordered organic material is regarded as a random resistor network (see **Figure 6b**). To address total electrical conductivity in disordered system, the initial is to obtain reference conductance Z and eliminate all conductive pathways between sites i and j with $Z_{ij} < Z$. Conductance between sites i and j is given by $Z_{ij} \propto \exp(-S_{ij})$ with [38]:

$$S_{ij} = 2\alpha R_{ij} + \frac{|E_i - E_f| + |E_j - E_f| + |E_i - E_j|}{2k_B T}.$$ (16)

The density of bonds $P(Z_m|E_i)$ then can be written as:

$$P(Z_m|E_i) = \int 4\pi R_{ij}^2 g(E_i)g(E_j)dR_{ij}dE_idE_j\theta(S_c - S_{ij}).$$ (17)

If the density of participating sites is P_s, then critical parameter S_c is found by solving equation:

$$P(Z_m|E_i) = B_c P_s = B_c \int g(E)dE\theta(S_c k_B T - |E - E_f|).$$ (18)

Based on numerical studies for three-dimensional amorphous system, the formation of infinite cluster corresponds to $B_c = 2.7$ [38]. By connecting Eqs. (16)–(18), bonds' density can be formulated as:

$$P(Z_m|E_i) = \frac{4\pi R^3}{3(2\alpha)^3} \times$$

$$\begin{cases} \int_{\epsilon_f}^{\epsilon_i} (S_c - \epsilon_j + \epsilon_f)^3 g(\epsilon_j)d\epsilon_j + \int_{\epsilon_i}^{S_c + \epsilon_f} (S_c - \epsilon_j + \epsilon_f)^3 g(\epsilon_j)d\epsilon_j + \int_{\epsilon_i - S_c}^{\epsilon_f} (S_c - \epsilon_i + \epsilon_j)^3 g(\epsilon_j)d\epsilon_j & \epsilon_i > \epsilon_f \\ \int_{\epsilon_i}^{\epsilon_f} (S_c + \epsilon_i - \epsilon_f)^3 g(\epsilon_j)d\epsilon_j + \int_{\epsilon_f - S_c}^{\epsilon_i} (S_c + \epsilon_i - \epsilon_f)^3 g(\epsilon_j)dE_j + \int_{\epsilon_f}^{\epsilon_i + S_c} (S_c - \epsilon_j + \epsilon_i)^3 g(\epsilon_j)d\epsilon_j & \epsilon_i < \epsilon_f \end{cases}$$ (19)

here ϵ is normalized energy as $\epsilon = \frac{E}{k_B T}$. This expression has been split into two regimes of $\epsilon_i > \epsilon_f$ and $\epsilon_i < \epsilon_f$, which are corresponding to contributions of ϵ_i above or below Fermi energy to $P(Z_m|E_i)$ and, therefore, Seebeck coefficient S, respectively. Above Fermi energy, charge carriers in shallow states will move by hopping to other shallow states. While below Fermi energy, charge carriers in deep states will move by thermal excitation to shallower states. By substituting Eqs. (13)–(15) and Eq. (19) into Eq. (8), one can obtain the final result of Seebeck coefficient.

Figure 7 shows simulated and experimental dependences of Seebeck coefficient on charge carriers' density; simulation is based on percolation theory, experimental data measured by using field-effect transistor (FET) from three kinds of conjugated polymers, that is, IDTBT, PBTTT and PSeDPPBT [39]. Model of percolation theory can reasonably reproduce experimental data under the whole range of charge carriers' density for different conjugated polymers.
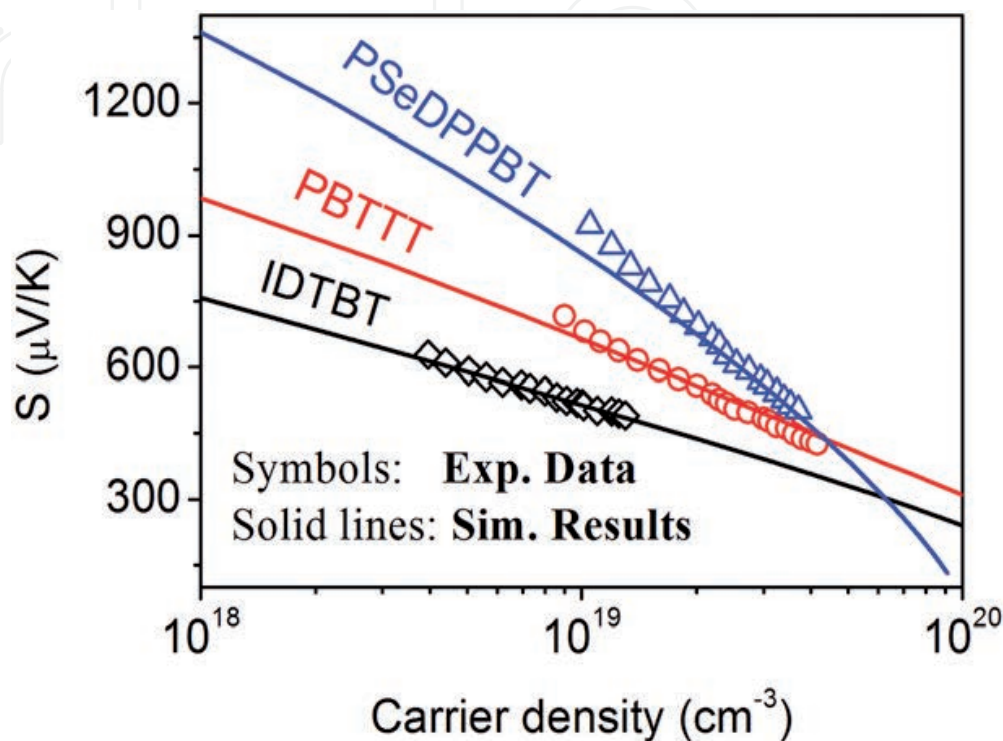

Figure 7. Charge carrier's density dependence of Seebeck coefficient for different materials at room temperature [37]. Symbols and solid lines are experimental and simulated results, respectively.

3.3. Hybrid model of Seebeck coefficient

Usual behavior of Seebeck coefficient is to decrease with increasing charge carriers' density. However, Germs et al. have observed unusual thermoelectric behavior for pentacene in TFT [40], indeed, at room temperature, increasing charge carriers' density results in expected decrease in S, while with decreasing temperature to values below room temperature, S demonstrates growth with increasing charge carriers' density at $T = 250$ K and even more pronounced at $T = 200$ K, as shown in **Figure 8**.

To explain this unusual thermoelectric behavior, Germs et al. developed simplified hybrid model that incorporates both variable-range hopping (VRH) and mobility edge (ME) transport [40]. Charge carrier and energy transport can be described independently by two processes: VRH-type process that occurs within exponential tail of localized states and band-like type transport that occurs within band-like states above mobility edge. Then, Seebeck coefficient of hybrid model is expressed as conductivity-weighted average of two contributing transport channels:

$$S = \frac{S_{ME}\sigma_{ME} + S_{VRH}\sigma_{VRH}}{\sigma_{ME} + \sigma_{VRH}}, \tag{20}$$

where S_{ME} and σ_{ME} are Seebeck coefficient and electrical conductivity in ME part, and S_{VRH} and σ_{VRH} are Seebeck coefficient and electrical conductivity in VRH part, respectively.

Then, general expression of Seebeck coefficient in Eq. (9) reduces:

$$S_{ME} = \frac{(E_c - E_f)}{eT} + A, \tag{21}$$

with

$$A = \frac{\int_0^\infty \frac{\varepsilon}{eT}\sigma(\varepsilon)d\varepsilon}{\int_0^\infty \sigma(\varepsilon)d\varepsilon}, \tag{22}$$

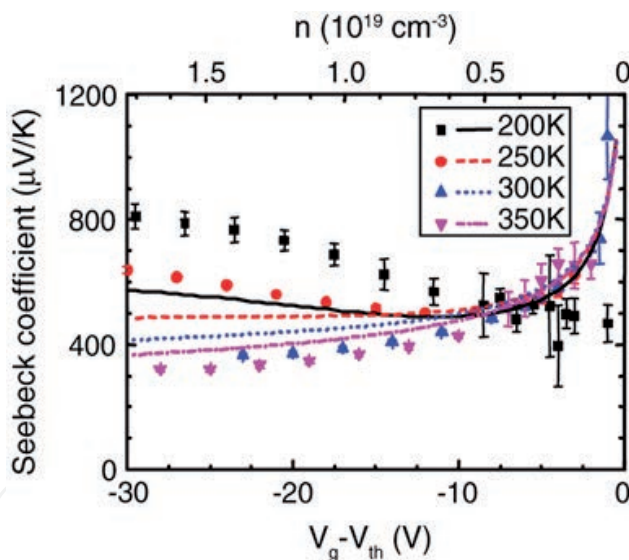where $\varepsilon = E - E_c$, E_c is energy value at mobility edge.

Figure 8. Measurements (symbols) and calculation (lines) of Seebeck coefficient as function of gate bias in pentacene TFT. Gate voltage V_g is corrected for threshold voltage V_{th} of TFT.

In Eq. (21), A accounts for excitations beyond the band edge with 1–20% of S_{ME}. Similarly, within VRH model, it is assumed that transport is determined by hopping event from equilibrium energy state to relatively narrow transport energy E^* [41], and Eq. (9) becomes:

$$S_{VRH} = \frac{(E^* - E_f)}{eT}, \tag{23}$$

Electrical conductivity in ME part is calculated as:

$$\sigma_{ME} = en_{free}\mu_{free}(T), \tag{24}$$

with power law dependence on temperature, $\mu_{free}(T) = \mu_0 T^{-m}$.

VRH part is described by Mott-Martens model that assumes transport to be dominated by hops from Fermi energy to transport level E^*. Electrical conductivity in VRH part is subsequently calculated by optimizing Miller-Abrahams expression as:

$$\sigma_{VRH} = \sigma_0 \exp\left[-2\alpha R^* - \frac{(E^* - E_f)}{k_B T}\right], \tag{25}$$

where position of transport level E^* and typical hopping distance R^* is connected via percolation argument:

$$B_c = \frac{4}{3}\pi(R^*)^3 \int_{E_f}^{E^*} g(E)dE, \tag{26}$$

where $B_c = 2.8$ is critical number of bonds, $g(E)$ represents DOS, which here is simplified to single exponential trap tail below mobility edge and constant density of extended states above E_c:

$$g(E) = \begin{cases} \dfrac{n_{trap}}{k_B T_0} \exp\left(-\dfrac{E}{k_B T_0}\right) & for\ E < E_c \\ \dfrac{n_0}{k_B T_0} & for\ E \geq E_c \end{cases} \quad (E_c = 0), \tag{27}$$

where n_0 is divided by $k_B T_0$ for dimensional reasons. The number of charge carriers above E_c, n_{free} follows from Fermi-Dirac distribution.

Figure 9 shows measured and calculated dependences of Seebeck coefficient on difference between gate voltage V_g and threshold voltage V_{th} on TFT at T = 200 K. One can see that at 200 K heat transported at mobility edge ($E_c - E_f$) and heat transported at transport level ($E^* - E_f$) both decrease with increasing charge carriers' density, accounting for downward trends in S_{ME} and S_{VRH}. Consequently, weight-averaged Seebeck coefficient S_{Hyb} shifts from S_{VRH} values at small gate bias up toward S_{ME} for large gate bias. Relatively large value of S_{ME} at lower temperatures follows from Eq. (21) and temperature independence of E_C.

3.4. Monte Carlo simulation

As compared with numeric model, analytical thermoelectric transport models exhibit more context and physical property, but they also have inevitable shortcoming due to the use of plenty of free parameters during simulation and calculation. In order to eliminate these hindrances, universal method has been used based on Monte Carlo (MC) simulation for describing hopping transport and insuring validity and accuracy of thermoelectric transport.
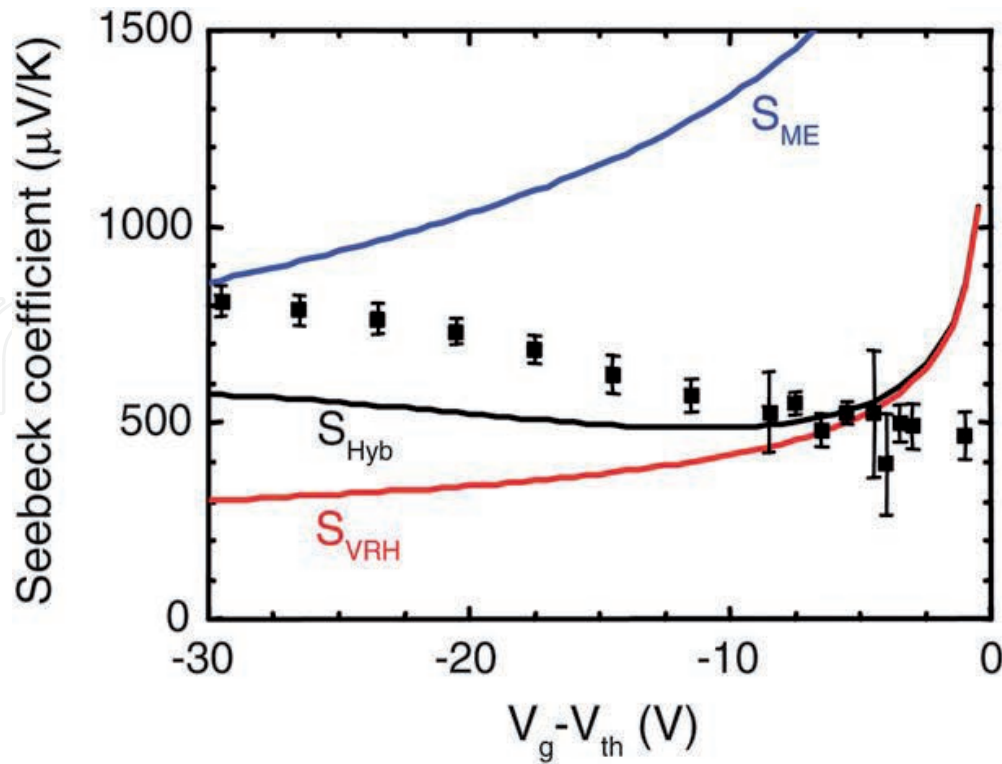
Figure 9. Measured (symbols) and calculated (lines) dependences of Seebeck coefficient on gate bias at T = 200 K [40]. S_{Hyb} is conductivity-weighted average of S_{VRH} and S_{ME}.

Kinetic Monte Carlo simulation generally includes six steps as follows [42]:

i. Initializing site energy E_i. Random energy E_i at site i derives from Gaussian or exponential DOS.

ii. Initial placement of charge carriers. Fermi-Dirac occupation probabilities will be used in randomly placing N_{ch} charge carriers.

iii. Choosing hopping events. If neglecting the polaron effect, hopping rates ν_{uuo} from site i to site j are based on Miller-Abrahams expression in Eq. (1). Corresponding setting is: (a) hopping rates equal to 0 to prevent hopping into already occupied sites; (b) introducing cut-off distance and set $\nu_{uuo} = 0$ for jumps longer than this distance.

Otherwise, renormalizing hopping rates Γ_{ij} as $p_{ij} = \dfrac{\Gamma_{ij}}{\sum\limits_{i',j'}\Gamma_{i'j'}}$. Sum of rates includes only

jumps from occupied to unoccupied sites, that is, $\Gamma_{ij} = 0$ for occupied site j or unoccupied site i. For every pair ij, index k (i.e., $ij \rightarrow k$ and $p_{ij} = p_k$), where $k \in \{1, ..., k_{max}\}$ with k_{max} being total number of all possible hopping events. Then, partial sum S_k is defined for every index k:

$$S_k = \sum_{k'=1}^{k} p_{k'}. \tag{28}$$

Apparently, for every k, extent from interval $[S_{k-1}, S_k]$ equals to probability p_k for k^{th} jump, and total extent of all intervals equals to 1, for example $S_{kmax} = 1$. Then, determining a

random real number r from interval [0, 1] and finding index k, here $S_{k-1} << r << S_k$, and one can find hopping event. After determining hoping event, one would move charge carrier between corresponding sites i and j.

iv. Calculation of waiting time. After finding each hopping transport, total simulation time t and waiting time τ would be added that has passed until the event took place. This time is determined by describing a random number from exponential waiting time distribution $P(\tau) = v_i \exp(-v_i \tau)$ with $v_i = \sum_j v_{ij}$ being the total rate for charge carrier hopping from site i. It is, therefore, written as:

$$\tau = \frac{-1}{v_i} \ln(x), \tag{29}$$

where random number x is drawn from interval [0, 1].

v. Calculating current density. Every time, when predefined numbers of jumps have occurred, current density $J(t)$ can be expressed as:

$$J(t) = \frac{e(N^+ - N^-)}{t N_y N_z a^2}, \tag{30}$$

where N^+ and N^- are the total number of jumps in and opposite direction of electric field for cross-sectional slice in yz plane, and a is lattice constant.

vi. Calculating Seebeck coefficient. Seebeck coefficient is given by expression as in Eq. (10), where transport energy is defined as averaged energy weighted by electrical conductivity distribution:

$$E_{trans} = \frac{\int E\sigma(E, T)\left(-\frac{\partial f}{\partial E}\right) dE}{\sigma(T)}, \tag{31}$$

with $\sigma(T) = \int \sigma(E, T)\left(-\frac{\partial f}{\partial E}\right) dE$.

Although kinetic MC technique gives a direct simulation of thermoelectric transport in organic semiconductor materials and, therefore, it is accurate for the most description of electronic conductivity, its negative factor is to require extensive computational resources, which leads to difficultly analyze and fit experimental data. **Figure 10** shows comparison of analytical model with MC simulation for Seebeck coefficient [42]. It is seen in **Figure 10**, that results exhibit qualitative agreement for all values of parameter α. For large α in **Figure 10a**, S_{sa} and S_{MC} show not only qualitative, but even relatively good quantitative agreement in energy interval $E < 0$ (corresponding to relative charge carriers' concentration $n/N_0 < 0.5$). For higher energies (and thus for higher concentrations), difference between S_{sa} and S_{MC} increases. As parameter α decreases, functional dependencies S_{sa} and S_{MC} remain very close to each other, but S_{sa} gets shifted with respect to S_{MC} (**Figure 10b**).
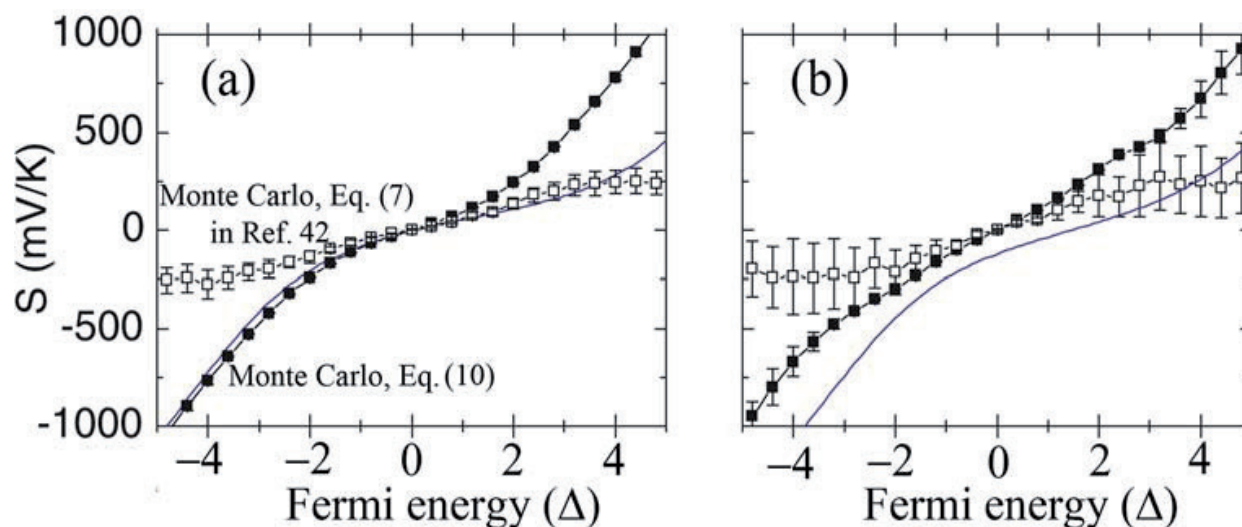
Figure 10. Monte Carlo and semi-analytical calculations of Seebeck coefficient for different values of localization length (a) $\alpha^{-1} = 1$ nm and (b) $\alpha^{-1} = 0.2$ nm. E_f is in units of $\varDelta$, $\varDelta = 4k_BT$ and T = 300 K.

3.5. First-principle calculation theory

First-principle (*ab initio*) theory would be deemed to the best type of theory for hopping charge transport in organic semiconductors, since it starts from particular chemical and geometrical structure of the system, and it starts directly at the level of established science and does not make assumptions, such as empirical model and fitting parameters. So far, a few researches on charge carriers transport properties based on first-principle theory are hardly beyond the scope of crystalline. Otherwise, direct calculation of Seebeck coefficient is hardly realistic. Current method combines generally first-principle calculations with transport theory. For example, Gao et al. have investigated theoretically Seebeck coefficient of narrow bandgap crystalline polymers, including crystalline solids β-Zn_4Sb_3 and $AuIn_2$ and these polymers, based on muffin-tin orbital and full-potential linearized augmented plane-wave (FLAPW) electronic structure code [43]. In essence, Gao et al.'s method for calculation of transport properties of crystalline solid is firstly based on semiclassical Boltzmann theory, following as:

$$\sigma_0(T) = \frac{e^2}{3}\int \tau(E,T)N(E)v^2(E)\left(-\frac{\partial f(E)}{\partial E}\right)dE, \tag{32}$$

where e, τ, f and v represent free electron charge, electronic relaxation time, Fermi-Dirac distribution function and Fermi velocity, respectively. If relaxation time for electron scattering processes is assumed to be constant, that is, $\tau(E,T) = $ const, which may yield reasonable simulated results in a wide range of materials, then temperature dependence of $\sigma_0(T)$ can be simulated based on constant relaxation time τ:

$$\frac{\sigma_0(T)}{\tau} = \frac{e^2}{3}\int N(E)v^2(E)\left(-\frac{\partial f(E)}{\partial E}\right)dE. \tag{33}$$

Then, Seebeck coefficient is calculated from ratio of the zeroth and first moments of electrical conductivity with respect to energy:

$$S(T) = \frac{1}{eT} \times \frac{I^1}{I^0}, \tag{34}$$

where

$$I^x(T) = \int \tau(E, T) N(E) v^2(E) (E - E_f)^x \left(-\frac{\partial f(E)}{\partial E} \right) dE. \tag{35}$$

Product of the density of states $N(E)$ and arbitrary quantity g, which is relative to energy and k-vector as in Eqs. (33) and (35), can be calculated by using integration on constant energy surface S in k space. Electronic band structure can be calculated by using WIEN97 and WIEN2K FLAPW [44] or pseudopotential plane-wave code in Vienna *ab initio* simulation package (VASP) [45].

Figure 11a and **b** shows simulated energy band structure of polythiophene polymer. Here, internal structural parameters of the polymer are fully optimized, and electronic band structure is calculated by pseudopotential plane-wave calculations employing ultrasoft Vanderbilt pseudopotential and generalized gradient scheme. Simulated results display that band structure of polythiophene is very simple, which exhibits semiconductor performance with band gap of 0.9 eV. Neutral polythiophene is electrical insulator. Otherwise, by inspecting band structure, one can find that, except very close to zone center, where the density of states is high, band dispersions are considerable. The special band structure, thus, induces very low value of Seebeck coefficient (~20 μV/K), as shown in **Figure 11**.
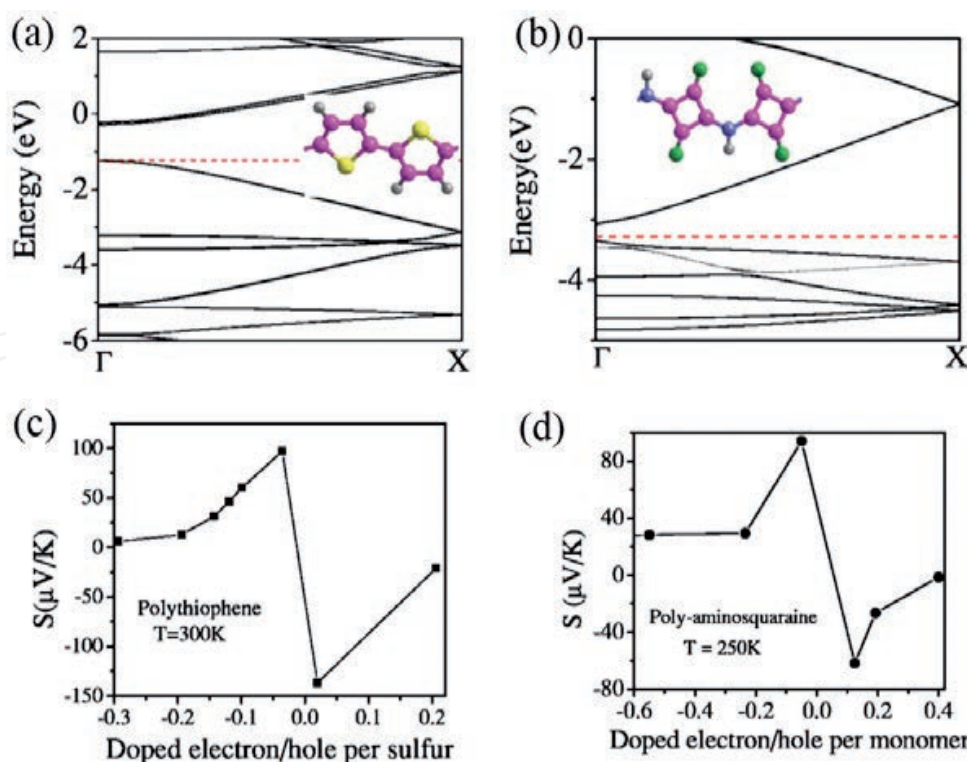

Figure 11. Calculated energy band structure (a), (b), and Seebeck coefficient (c), (d), for polythiophene (left) and polyaminosquarine (right), respectively [43]. Isolated planar polymer chains were used for this calculation.

Similar to calculated method from Gao et al., Shuai et al. have combined first-principles band structure calculations and Boltzmann transport theory to study thermoelectric in pentacene and rubrene crystals [46]. Electronic contribution to Seebeck coefficient is obtained in approximations of constant relaxation time and rigid band, as shown in **Figure 12**. Calculation results exhibited also the similar trend compared with experimental Seebeck coefficient.
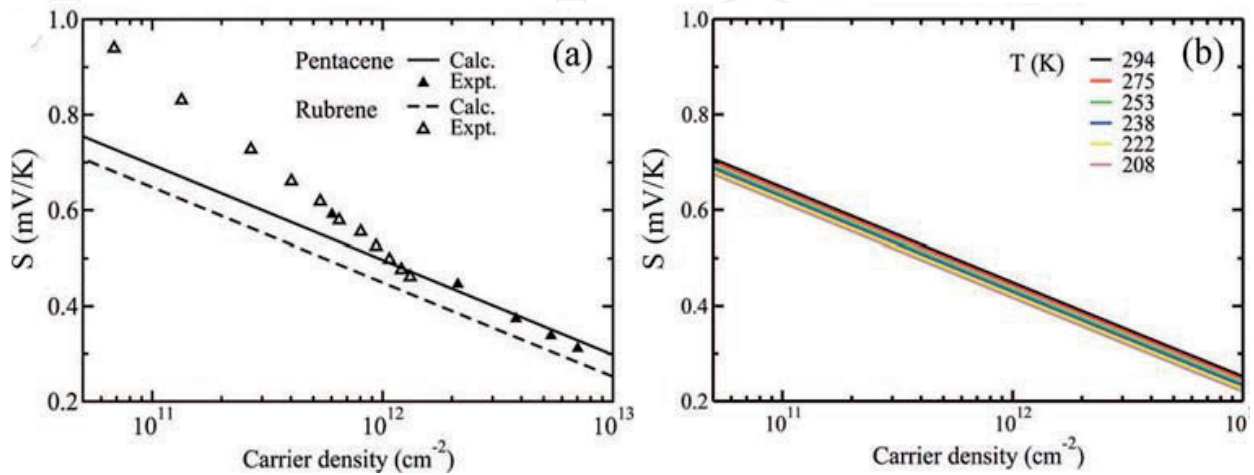

Figure 12. Seebeck coefficient calculated as function of charge carrier's concentration (a) for pentacene and rubrene at room temperature and compared to FET measurements. Calculated Seebeck coefficients have been averaged over three crystal directions (b) for rubrene at temperature in the range between 200 and 300 K [46].

Afterward, Shuai et al. applied also combining method to calculate thermoelectric properties of organic materials, which is used to calculating α-form phthalocyanine crystals H2Pc, CuPc, NiPc and TiOPc [47]. This combining method includes first-principles band structure calculations, Boltzmann transport theory and deformation potential theory. They used first-principles calculations in VASP to calculate Seebeck coefficient. After obtaining band structure, Boltzmann transport theory was performed to calculate properties related to charge carrier transport, as in Eqs. (32) and (33).

Being different from Gao et al.'s and Shuai et al.'s previous works, it is assumed that relaxation time is a constant, which can be estimated by deformation potential theory for treating electron-phonon scattering. In terms of corresponding articles [46, 48], acoustic phonon scattering in both pristine and doped system was simulated by this theory including scattering matrix element for electrons from $\mathbf{k}$ state to $\mathbf{k}'$ state expressing as:

$$|M(\mathbf{k},\mathbf{k}')|^2 = \frac{E_1^2}{C_{ii}}k_B T, \tag{36}$$

where E_1 is deformation potential constant that represents energy band shift caused by crystal lattice deformation, and C_{ii} is elastic constant in the direction of lattice wave's propagation. Then, relaxation time can be expressed by scattering probability:

$$\frac{1}{\tau(i,k)} = \sum_{k' \in BZ} \left\{ \frac{2\pi}{\hbar} |M(\mathbf{k},\mathbf{k}')|^2 \delta[\varepsilon(i,k) - \varepsilon(i,k')](1 - \cos\theta) \right\}, \tag{37}$$

where $\delta[\varepsilon(i,k)-\varepsilon(i,k')]$ is Dirac delta function, and θ is angle between $\mathbf{k}$ and $\mathbf{k}'$. In Bardeen and Shockley's method, scattering is assumed to be isotropic, and matrix element of interactions $M(\mathbf{k},\mathbf{k}')$ is not relative with $\mathbf{k}$ and $\mathbf{k}'$.

Calculated dependences of Seebeck coefficient on charge carriers' concentration are shown in **Figure 13**. Calculated dependences of Seebeck coefficient display different properties such as positive S values for holes and negative S values for electrons. Seebeck coefficient value is isotropic at first glance, and it decreases rapidly as charge carriers' concentration increases.
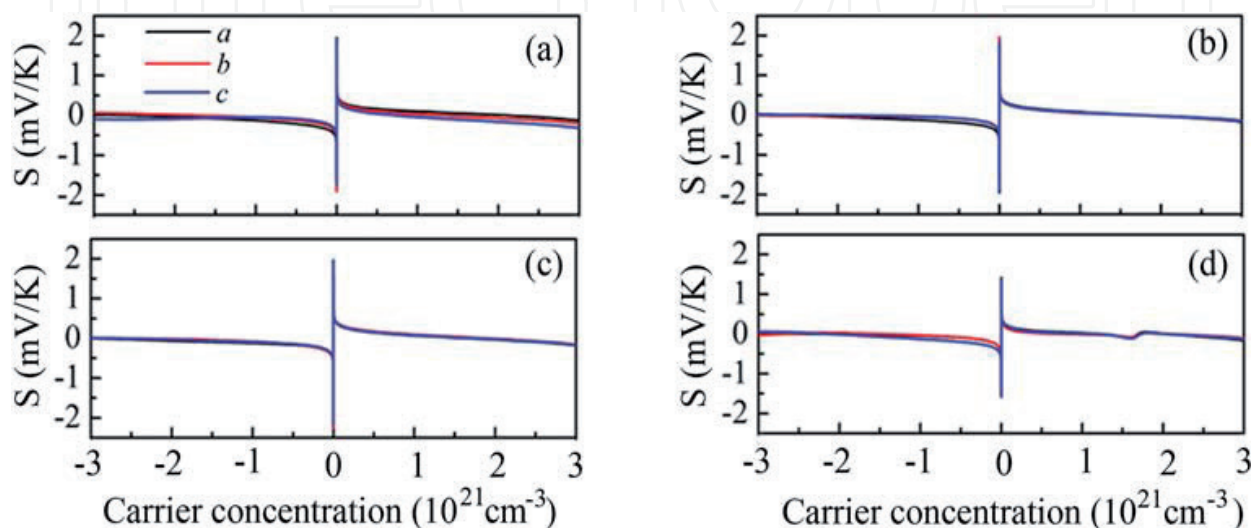

Figure 13. Seebeck coefficient for (a) H2Pc, (b) CuPc, (c) NiPc, (d) TiOPc calculated as a function of the charge carriers concentration at 298 K [47]. a, b and c denote a, b and c crystal axes, respectively.

4. Conclusion and outlook

In the past decades, the research on organic thermoelectric materials has made great progress. Rich variety of novel organic materials has been synthesized and applied in thermoelectric devices, and thermoelectric performances of organic semiconductors have been promoted greatly. However, as compared to inorganic thermoelectric materials, organic thermoelectric materials still exhibit lower ZT so far. However, situation looks like that progress in theoretical study of organic thermoelectric effect lags far behind experimental investigation in the last 30 years, but has been changed remarkably until the recent five years. Here, we have tried to describe organic thermoelectric materials and theoretical approaches, which allow to calculate characteristics of charge carrier transport processes responsible for thermoelectric effect in organic semiconductors. We hope that these contexts can be helpful to improve thermoelectric effect in organic materials and provide motivation for growth of thermoelectric applications of organic semiconductors. We believe that quest for green energy sources will stimulate intensive research and development works in the field of novel organic thermoelectric materials and devices that will result in serious improvement in thermoelectric efficiency of organic thermoelectric materials and enable development of novel high-performance and affordable organic thermoelectric devices.

Abbreviations

DOS	density of states
VRH	variable-range hopping,
PANI	polyaniline,
PPV	poly(p-phenylenevinylene),
PEDOT	poly(3,4-ethylenedioxythiophene),
PSS	poly(styrenesulfonate),
PMeOPV	poly(2,5-dimethoxy phenylenevinylene),
MEHPPV	poly[2-methoxy-5-(2-ethylhexyloxy)-1,4-phenylenevinylene],
P3HT	poly(3-hexylthiophene-2,5-diyl),
DMSO	dimethylsulfoxide,
EG	ethylene glycol,
S	Seebeck coefficient,
Π	Peltier coefficient,
TFT	thin film transistors,
PF	power factor,
FET	field-effect transistor,
ME	mobility edge,
V_g	gate voltage,
V_{th}	threshold voltage,
MC	Monte Carlo,
FLAPW	full-potential linearized augmented plane-wave,
VASP	Vienna ab initio simulation package.

Author details

Nianduan Lu*, Ling Li and Ming Liu

*Address all correspondence to: lunianduan@ime.ac.cn

Key Laboratory of Microelectronic Devices & Integrated Technology, Institute of Microelectronics of Chinese Academy of Sciences, Beijing, China

References

[1] Reese C, Roberts M, Ling M, Bao Z.: Organic thin film transistors. Mater. Today. 2004;**7** (9):20–27. doi:10.1016/S1369-7021(04)00398-0

[2] Elkington D, Cooling N, Belcher W, Dastoor PC, Zhou XJ.: Organic thin-film transistor (OTFT)-based sensors. Electronics. 2014;**3**:234–254. doi:10.3390/electronics3020234

[3] Lu ND, Li L, Liu M.: A review of carrier thermoelectric-transport in organic semiconductors. Phys. Chem. Chem. Phys. 2016;**18**:19503. doi:10.1039/C6CP02830F

[4] Owens RM, Malliaras GG.: Organic electronics at the interface with biology. MRS Bull. 2010;**35**(06):449–456. doi:10.1557/mrs2010.583

[5] Law KK.: Organic photoconductive materials: recent trends and developments. Chem. Rev. 1993;**93**(1):449–486. doi:10.1021/cr00017a020

[6] Shirakawa H, Louis EJ, MacDiarmid AG, Chiang CK, Heeger AJ.: Synthesis of electrically conducting organic polymers: halogen derivatives of polyacetylene, (CH)x. J. Chem. Soc. Chem. Commun. 1977;(16):578–580. doi:10.1039/C39770000578

[7] Chason M, Brzis PW, Zhang J, Kalyanasundaram K, Gamota DR.: Printed organic semiconductors devices. Proc. IEEE. 2006;**93**(7):1348–1356. doi:10.1109/JPROC.2005. 850306

[8] Li FM, Nathan F, Wu YL, Ong BS.: Organic thin film transistor integration: a hybrid approach. Wiley-Vch Verlag GmbH & Co. KGaA, Boshstr. Weinheim Germany; 2011. 270 pp. doi:10.1002/9783527634446

[9] Ito T. Shirakawa H, Ikeda S.: Simultaneous polymerization and formation of polyacetylene film on the surface of concentrated soluble Ziegler-type catalyst solution. J. Polym. Sci.: Polym. Chem. Ed. 1974;**12**(1):11–20. doi:10.1002/pol.1974.170120102

[10] Chiang CK, Fincher CB, Park JYW, Heeger AJ.: Electrical conductivity in doped polyacetylene. Phys. Rev. Lett. 1977;**39**(17):1098–1011.

[11] Minder NA, Ono S, Chen ZH, Facchetti A, Morpurgo AF.: Band-like electron transport in organic transistors and implication of the molecular structure for performance optimization. Adv. Mater. 2012;**24**:503–508. doi:10.1002/adma.201103960

[12] Novikov SV, Tyutnev AP.: Charge carrier transport in molecularly doped polycarbonate as a test case for the dipolar glass model. J. Chem. Phys. 2013;**138**:104120. doi:10.1063/1.4794791

[13] Tessler N, Preezant Y, Rappaport N, Roichman Y.: Charge transport in disordered organic materials and its relevance to thin-film devices: a tutorial review. Adv. Mater. 2009;**21**:2741–2761. doi:10.1002/adma.200803541

[14] Coropceanu V, Cornil J, Filho DS, Olivier Y, Silbey R, Brédas JL.: Charge transport in organic semiconductors. Chem. Rev. 2007;**107**:926–952. doi:10.1021/cr050140x

[15] Li L, Meller G, Kosina H.: Carrier concentration dependence of the mobility in organic semiconductors. Syn. Metals. 2007;**157**:243–246. doi:10.1016/j.synthmet.2007.03. 002

[16] Arkhipov VI, Adriaenssens GJ.: Trap-controlled dispersive transport in systems of randomly fluctuating localized states. Philos. Mag. B. 1997;**76**(1):11–22. doi:10.1080/01418639708241075

[17] Lu ND, Li L, Banerjee W, Sun PX, Gao N, Liu M.: Charge carrier hopping transport based on Marcus theory and variable-range hopping theory in organic semiconductors. J. Appl. Phys. 2015;**118**:045701. doi:10.1063/1.4927334

[18] Miller A, Abrahams E.: Impurity conduction at low concentrations. Phys. Rev. 1960;**120**:745. doi:10.1103/PhysRev.120.745

[19] Mott NF, Davis EA. Electronic Processes in Non-Crystalline Materials. 2nd ed. Oxford: Oxford University Press; 1971. 32 p.

[20] Li L, Lu ND, Liu M.: Field effect mobility model in oxide semiconductor thin film transistors with arbitrary energy distribution of traps. IEEE Electron Dev. Lett. 2014;**35** (2):226. doi:10.1109/LED.2013.2291782

[21] Bubnova O, Khan ZU, Malti A, Braun S, Fahlman M, Berggren M, Crispin X.: Optimiza-tion of the thermoelectric figure of merit in the conducting polymer poly(3,4-ethylene-dioxythiophene). Nat. Mater. 2011;**10**:429–433. doi:10.1038/nmat3012

[22] Weathers A, Khan ZU, Brooke R, Evans D, Pettes MT, Andreasen JW, Crispin X, Shi L.: Significant electronic thermal transport in the conducting polymer poly(3,4-ethylenediox-ythiophene). Adv. Mater. 2015;**27**:2101–2106. doi:10.1002/adma. 201404738

[23] Culebras M, Gómez CM, Cantarero A.: Review on polymers for thermoelectric applica-tions. Materials. 2014;**7**:6701–6732. doi:10.3390/ma7096701

[24] Zhang Q, Sun YM, Xu W, Zhu DB.: Organic thermoelectric materials: emerging green energy materials converting heat to electricity directly and efficiently. Adv. Mater. 2014;**26**:6829–6851. doi:10.1002/adma.201305371

[25] Wei QS, Mukaida M, Kirihara K, Naitoh Y, Ishida T.: Recent progress on PEDOT-based thermoelectric materials. Materials. 2015;**8**:732–750. doi:10.3390/ma8020732

[26] Sun YM, Sheng P, Di CG, Jiao F, Xu W, Qiu D, Zhu DB.: Organic thermoelectric materials and devices based on p- and n-type poly(metal 1,1,2,2-ethenetetrathiolate)s. Adv. Mater. 2012;**24**:932. doi:10.1002/adma.201104305

[27] Kim GH, Shao L, Zhang K, Pipe KP.: Engineered doping of organic semiconductors for enhanced thermoelectric efficiency. Nat. Mater. 2013;**12**:719–723. doi:10.1038/nmat3635

[28] Harada K, Sumino M, Adachi C, Tanaka S, Miyazaki K.: Improved thermoelectric perfor-mance of organic thin-film elements utilizing a bilayer structure of pentacene and 2,3,5,6-tetrafluoro-7,7,8,8 -tetracyanoquinodimethane(F4-TCNQ). Appl. Phys. 2010;**96**:253304. doi:10.1063/1.3456394

[29] Minakata T, Nagoya I, Ozaki M.: Highly ordered and conducting thin film of pentacene doped with iodine vapor. J. Appl. Phys. 1991;**69**:7354. doi:10.1063/1.347594

[30] Cutler M, Mott NF.: Observation of Anderson localization in an electron Gas. Phys. Rev. 1969;**181**:1336.

[31] Nagel P. Electronic transport in amorphous semiconductors. In: Brodsky MH, editor. Amorphous Semiconductors. Springer-Verlag: Springer Berlin Heidelberg; 1979. pp. 113–158. doi:10.1007/3-540-16008-6_159

[32] Fritzsche H.: A general expression for the thermoelectric power. Solid State Commun. 1971;**9**:1813–1815.

[33]   Schmechel R.: Hopping transport in doped organic semiconductors: a theoretical approach and its application to p-doped zinc-phthalocyanine. J. Appl. Phys. 2003;**93**:4653–4660. doi:10.1063/1.1560571

[34]   Ziman JM.: The localization of electrons in ordered and disordered systems I. Percolation of classical particles. J. Phys. C. 1968;**1**:1532–1538.

[35]   Shante VKS, Kirkpatrick S.: An introduction to percolation theory. Adv. Phys. 1971;**20**:325–357.

[36]   Kirkpatrick S.: Classical transport in disordered media: scaling and effective-medium theories. Phys. Rev. Lett. 1971;**27**:1722–1725.

[37]   Lu ND, Li L, M. Liu.: Universal carrier thermoelectric-transport model based on percolation theory in organic semiconductors. Phys. Rev. B. 2015;**91**:195205. doi:10. 1103/ PhysRevB.91.195205

[38]   Limketkai BN, Jadhav P, Baldo MA.: Electric-field-dependent percolation model of charge-carrier mobility in amorphous organic semiconductors. Phys. Rev. B. 2007;**75**:113203. doi:10.1103/PhysRevB.75.113203

[39]   Venkateshvaran D, Nikolka M, Sadhanala A, Lemaur V, Zelazny M, Kepa M, Hurhangee M, Kronemeijer AJ, Pecunia V, Nasrallah I, Romanov I, Broch K, McCulloch I, Emin D, Olivier Y, Cornil J, Beljonne D, Sirringhuas H.: Approaching disorder-free transport in high-mobility conjugated polymers. Nature. 2014;**515**:384–388. doi:10.1038/nature13854

[40]   Germs WC, Guo K, Janssen RAJ, Kemerink M.: Unusual thermoelectric behavior indicating a hopping to bandlike transport transition in pentacene. Phys. Rev. Lett. 2012;**109**:016601. doi:10.1103/PhysRevLett.109.016601

[41]   Baranovskii SD, Faber T, Hensel F, Thomas P.: The applicability of the transport-energy concept to various disordered materials. J. Phys. Condens. Matter. 1997;**9**:2699–2706.

[42]   Ihnatsenka S, Crispin X, Zozoulenko IV.: Understanding hopping transport and thermoelectric properties of conducting polymers. Phys. Rev. B. 2015;**92**:035201. doi:10.1103/ PhysRevB.92.035201

[43]   Gao X, Uehara K, Klug DD, Patchkovskii S, Tse JS, Tritt TM.: Theoretical studies on the thermopower of semiconductors and low- band-gap crystalline polymers. Phys. Rev. B. 2005;**72**:125202. doi:10.1103/PhysRevB.72.125202

[44]   Perdew JP, Burke K, Ernzerhof M.: Generalized gradient approximation made simple. Phys. Rev. Lett. 1996;**77**:3865.

[45]   Kresse G, Furthmuller J.: Efficiency of ab-initio total energy calculations for metals and semiconductors using a plane-wave basis set. Comput. Mater. Sci. 1996;**6**:16–50. doi:10.1016/0927-0256(96)00008-0

[46]   Wang D, Tang L, Long MQ, Shuai ZG.: First-principles investigation of organic semiconductors for thermoelectric applications. J. Chem. Phys. 2009;**131**:224704. doi:10.1063/ 1.3270161

[47] Chen JM, Wang D, Shuai ZG.: First-principles predictions of thermoelectric figure of merit for organic materials: deformation potential approximation. J. Chem. Theory Comput. 2012;**8**:3338–3347. doi:10.1021/ct3004436

[48] Shi W, Zhao TQ, Xi JY, Wang D, Shuai ZG.: Unravelling doping effects on PEDOT at the molecular level: from geometry to thermoelectric transport properties. J. Am. Chem. Soc. 2015;**137**:12929–12938. doi:10.1021/jacs.5b06584